Optical Pumping of Rubidium

Janet Chao, Dean Henze, Patrick Smith, Kent Lee

April 7, 2013

Abstract

Optical pumping was used in order to determine the Lande g-factor g_f and the related nuclear spin, $\vec{I}$, of two isotopes of Rubidium, ^{85}Rb and ^{87}Rb, by examining the Zeeman splitting of the hyperfine structure. Optical pumping was also used to examine the quadratic Zeeman effect.

1 INTRODUCTION

Although Albert Einstein laid down the theoretical foundations for the laser and maser in his paper *On the Quantum theory of Radiation* in 1917, it was not until 1950 when Alfred Kastler proposed the method of optical pumping that the development of the laser and maser could truly be possible. Brossel, Kastler, and Winter experimentally confirmed Kastler's method of optical pumping two years later and Kastler was awarded the Nobel Prize for Physics in 1966 "for the discovery and development of optical methods for studying hertzian resonances in atoms." Optical pumping is the process by which photons are used to raise the energy level states in an atom or molecule, redistributing them from thermodynamic equilibrium so that the majority of the atoms occupy a single energy state. The discovery of optical pumping has most notably been critical to the development of lazers and masers, but has also enhanced quantum theory by enhancing theories concerning Zeeman splitting, nuclear spins, and overall nuclear perturbation. Such theories have been significantly important to the development of technologies such as Nuclear Magnetic Resonance and Magnetic Resonance Imaging. This paper will utilize the method of optical pumping to experimentally determine the nuclear spin for two isotopes of Rubidium, ^{85}Rb and ^{87}Rb, beginning with an explanation of the theory behind optical pumping (Section 2), the experimental design and apparatus (Section 3), our results (Section 4), and a discussion of our conclusions (Section 5).

2 THEORY

This experiment uses rubidium atoms due to its single valence electron in the 5s that gives it structure as the hydrogen atom. In other words, all of rubidium's inner electrons are paired and located in full shells, allowing us to focus on the single outer valence electron and use a model that considers rubidium as though it is a simple hydrogenic single electron atom. Therefore, ^{85}Rb, ^{87}Rb and all other ground state alkali atoms can be represented by the spectroscopic notation of the electronic state $^2S_{\frac{1}{2}}$, which corresponds to orbital angular momentum $L = 0$, spin angular momentum $S = \frac{1}{2}$, and total non-nuclear angular momentum $J = \frac{1}{2}$ since

$$\vec{J} = \vec{L} + \vec{S}. \tag{1}$$

When the single valence electron of an alkali atom becomes excited into its first excited state, it can jump into the 5p orbital and into the P state. However, the P state can further split into $^2P_{\frac{1}{2}}$ and $^2P_{\frac{3}{2}}$ since J can have values of L+S and L-S only. The energy splitting between $^2P_{\frac{1}{2}}$ and $^2P_{\frac{3}{2}}$ entitled the Fine Structure is much smaller than the energy difference between the S and P state.

Now, taking into account the nucleus of the atom, we must consider the nuclear spin, I, and

Figure 1: A not-to-scale diagram of the fine structure splitting of an alkali atom valence electron

the total non-nuclear angular momentum, J in order to form a total angular momentum of the atom, F, where

$$\vec{F} = \vec{I} + \vec{J}. \quad (2)$$

When we account for the atom's nuclear spin as well, the total angular momentum of the atom's ground state can be split further into two levels. This splitting is known as the hyperfine splitting. For example, ^{85}Rb has a nuclear spin $I = \frac{5}{2}$, so that $F = 3, 2$ (since J can have values of L + S or L - S).
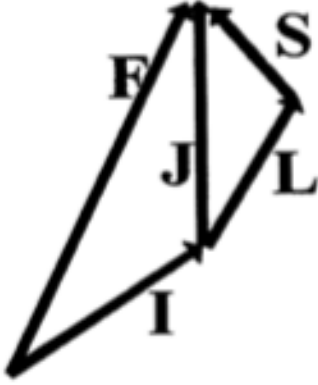

Figure 2: Vector model of the hyperfine coupling in an alkali atom

Furthermore, in the presence of a weak external magnetic field B, the Zeeman Effect can be produced in which the energy levels are even further split. When the electronic and nuclear magnetic moments interact with the external field, the magnetic field can actually split each F level into $2F + 1$ sublevels. The spacing between these splittings are determined by the direct interaction of the nuclear magnetic moment with the applied magnetic field, which can be utilized to observe all of the possible transitions. For example, the F=2 hyperfine splitting can be split into 5 (2F+1) different states

of $M_f = +2, +1, 0, 1, 2$ as shown in Figure 3. The Hamiltonian that describes the interaction of the electronic and nuclear magnetic moments with the external magnetic field is

$$H = h\alpha \vec{I}\vec{J} - \frac{\mu_J}{\vec{J}}\vec{J}\dot{\vec{B}} - \frac{\mu_I}{\vec{I}}\vec{I}\dot{\vec{B}}, \quad (3)$$

where $\vec{I}$ is the nuclear spin vector, $\vec{B}$ is the magnetic field vector, $\vec{J}$ is the total angular momentum vector, μ_J is the nuclear magnetic moment, and μ_J is the electronic magnetic moment. This is the Hamiltonian that accounts for the Zeeman splitting seen in Figure 3 and Figure 4.
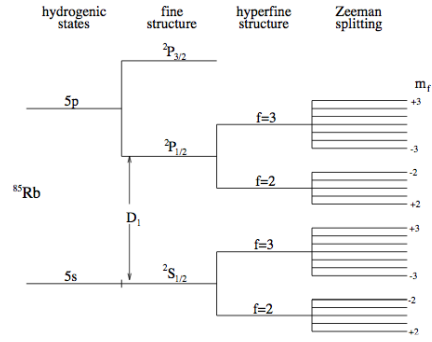

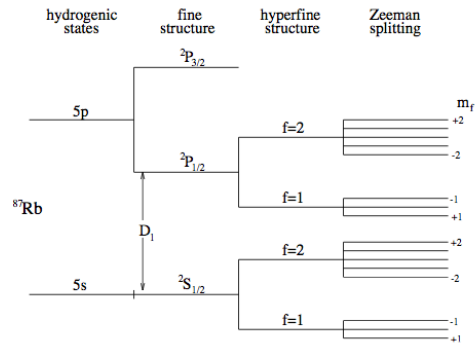Figure 3: Energy levels including Zeeman splittings of ^{85}Rb in a weak magnetic field (not to scale)

Figure 4: Energy levels including Zeeman splittings of ^{87}Rb in a weak magnetic field (not to scale)

By an approximation that ignores the nucleus, Equation 3 can be used to write the energy of the interaction of an atom with the external magnetic field as

$$E = -g_J \mu_0 M_f B, \qquad (4)$$

where $\mu_0 = 9.27 \times 10^{-24} \frac{J}{T}$ is the Bohn magneton, M_f is the component of the electron spin along the magnetic field, and $_J$ is the Lande g-factor represented by

$$g_J = \frac{(\vec{L} + 2\vec{S})\vec{J}}{J^2}. \qquad (5)$$

Equation 5 can then be evaluated from the vector model to be

$$g_J = 1 + \frac{J(J+1) + S(S+1) - L(L+2)}{2J(J+1)}. \qquad (6)$$

When we consider the nucleus, the nucleus-considering g-factor, g_F, can be expressed as

$$g_F = g_J \frac{F(F+1) + J(J+1) - I(I+1)}{2F(F+1)}. \qquad (7)$$

The interaction energy (W) which now also considers the nucleus can be expressed as

$$W = g_F \mu_o M_f B. \qquad (8)$$

Experiment 1 uses weak Zeeman Effects and these theories explained previously (particularly Equations 6, 7, and 8) in order to determine g_F and thereby I for both ^{85}Rb and ^{87}Rb. The method in doing so will be described further in the Experimental Design section.

The weak Zeeman results are only satisfactory when the interaction with the magnetic field is small so that the energy levels depend only linearly on the magnetic field. When the atoms become exposed to large magnetic fields, the quadratic Zeeman effect is observed where I and J begin to decouple and the quantum mixing of the states must be taken into account. The quadratic Zeeman interaction energy can be described the the Breit-Rabi equation

$$W(F, M_f) = -\frac{\Delta W}{2(2I+1)} - \frac{\mu_I}{I} B M_F \pm \frac{\Delta W}{2} [1 + \frac{4M_F}{2I+1} x + x^2]^{1/2} \qquad (9)$$

where

$$x = (g_J - g_I) \frac{\mu_0 B}{\Delta W} \qquad (10)$$

and

$$g_I = -\frac{\mu_I}{I \mu_I}. \qquad (11)$$

W is the interaction energy and ΔW is the hyperfine energy splitting. In a simplified version of the Breit-Rabi equation shown in Figure , the $\frac{\mu_I}{I} B M_F$ term in Equation 9 and the g_I term in Equation 10 are considered negligible and omitted. As seen in Figure 5, at regions near x=0,
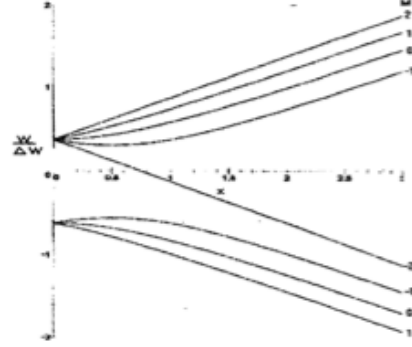

Figure 5: Breit-Rabi diagram of the ground state ^{85}Rb where the nuclear spin I is 3/2 and the nuclear magnetic moment μ_J is positive

the energy level splitting is linearly related to the applied magnetic field. At the intermediate region, the splitting becomes quadratic. Then as x values increase towards the end of the curve in a region known as the Paschen-Back region, the energy levels become linear once again. This linearity at the Paschen-Back region occurs because I and J decouple so that the upper four levels correspond to $m_J = 1/2$ and the lower four levels correspond to $m_J = -1/2$. In the intermediate, non-linear region, the energy levels are quadratic as I and J are decoupling and M_J is no longer a "good" quantum number since its components m_I and m_J are
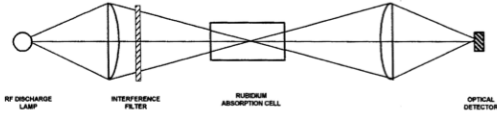
Figure 6: Optical pumping apparatus arrangement

separating and becoming more distinct. This can be seen because

$$M_J = m_I + m_J. \tag{12}$$

This quadratic Zeeman effect is observed in Experiment 2 of this experiment and will be further discussed in the Experimental Design section.

3 EXPERIMENTAL DESIGN

This apparatus used in these experiments consists of a rubidium discharge lamp, an interference filter, a rubidium absorption cell, and an optical detector arranged as shown in Figure 6 along with Helmholtz coils and an radiofrequency source. The rubidium discharge lamp emits photons of light which pass through the interference filter. The interference filter allows photons at wavelengths of 795 nm through, while selectively blocking out photons at wavelengths of 780 nm. The 795 nm wavelength photons then pass through a linear polarizer and quarter wave plate. The linear polarizer polarizes the light so that only clockwise rotating light goes through. Once this light reaches the rubidium absorption cell, it interactions with the Rubidium atoms, exciting them from the $^2S_{1/2}$ state to the $^2P_{1/2}$ state. The rubidium absorption cell also contains inert Xenon gas molecules. Since the Xenon atoms have a full valence shell, they do not react with the Rubidium atoms, but rather act as a buffer by providing elastic collisions with the rubidium atoms that prevent the rubidium from colliding into the walls of the cell and destroying their optical pumping. When a weak external magnetic field is applied, the hyperfine energy levels become further split by the Zeeman Effect. The previous clockwise polarization of the light

by the linear polarizer only allows $\Delta M_F = +1$ transitions to occur within a F state hyperfine splitting. Because of this selection rule, electrons in both the $^2S_{1/2}$ state and the $^2P_{1/2}$ state will be able to pump their electrons in their higher M_F states. As discussed in the previous Theory section, there are 2F+1 number of M_F states. For ^{87}Rb atoms after constant firing of photons by the light source, all atoms should become stuck at the ground state $^2S_{1/2}$ $M_F = 1$ Zeeman level. This is known as the "dark state" because these electrons have nowhere else to go. Atoms in the $^2P_{1/2}$ substates can move up the Zeeman energy levels and also reemit a photon to fall back down to the $^2S_{1/2}$ ground state. Similarly, populations of atoms in the $M_F = -1$ and $M_F = 0$ substates in the $^2S_{1/2}$ ground state can undergo a $\Delta M_F = +1$ transition and can also absorb light to reach the excited $^2P_{1/2}$ level. However, at the ground state $^2S_{1/2}$ $M_F = +1$ Zeeman level, the highest M_F level of the ground state, have nowhere else to go and remain stuck there since they cannot be reemitted nor absorbed into a higher or lower substate or state. Therefore, the electrons in a population of atoms can be pumped into the highest M_F level of the ground state by repeated absorption and reemission of photons until eventually all the atoms end up in the $M_F = +1$ Zeeman level of the F=1 hyperfine structure. This process occurs similarly in ^{85}Rb except that all the atoms would end up in the $M_F = +2$ Zeeman level of F=2 in the ground state, since this is the highest ground state level for the hyperfine structure of F=2. When most of the population of rubidium atoms reaches the dark state, light will no longer be absorbed by the rubidium absorption cell and the optical detector will detect a maximum peak of intensity.

The magnetic field in this experiment is applied by Helmholtz coils. All coils are perpendicular to each other and the vertical and horizontal coils are used to get rid of any external magnetism outside the apparatus. Furthermore, experimental setup of the apparatus contributes to getting rid of external magnetism by aligning the apparatus along the earth's magnetic field. The sweep coil is set to sweeps

through a range of determined magnetic magnitudes. The radiofrequency source is used to provide energy to the atoms, causing a decay of M_f levels that allows optical pumping to be disturbed and to take electrons out of the dark state, which causes a dip in the optical detector's reading.

4 RESULTS

4.1 Weak Zeeman Effects

In the weak Zeeman experiment, we sought to determine the lande g-factor and the nuclear spin for ^{87}Rb and ^{85}Rb. We began by canceling out all external magnetic fields and sweeping through a range of B values to see where optical pumping is destroyed and therefore where B field = 0 (corresponds to a dip in the oscilloscope reading). Then, for RF frequencies between 50 KHz and 150 KHz (in increments of 10 KHz), we swept through the magnetic field range to find dips for the ^{85}Rb and ^{87}Rb atoms. We then observed these dips are different frequencies and recorded the corresponding voltage dips that occured with each frequency. Since the resistance was 1 ohm and $V = IR$, the current was the same value as the voltage. We then used the equation

$$B = 8.991 \times 10^-3 \frac{IN}{\vec{R}}$$

to calculate the value of B for the dips from current (I) and graphed B and frequency accordingly to find the slope. After determining the slope, we could use Equation 8 where $W = h\gamma$ and rearrange it so that

$$\frac{B}{\gamma} = \frac{h}{g_F \mu_0}. \quad (14)$$

Since the slope corresponds to $\frac{B}{\gamma}$ and the manual tells us that $\frac{m u_0}{h} = 1.3996$ MHz, we were able to determine that $g_F = 0.093$ for ^{87}Rb and $g_F = 0.14$ for ^{85}Rb. Using Equation 6 and Equation 7, we can then determine the value of I.

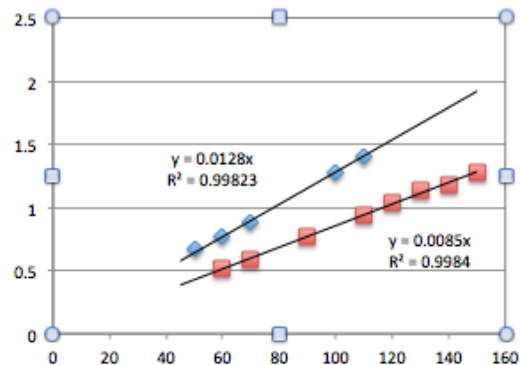Figure 7: Frequencies (in KHz) and corresponding magnetic field dips for ^{87}Rb (blue) and ^{85}Rb (red)

4.2 Quadratic Zeeman Effects

The goal of this portion of the experiment was to observe the quadratic Zeeman effect and to record the B value at which a given RF value destroys optical pumping. We swept the magnetic field through a range of larger B fields and observed dips as showns in Figure 8.
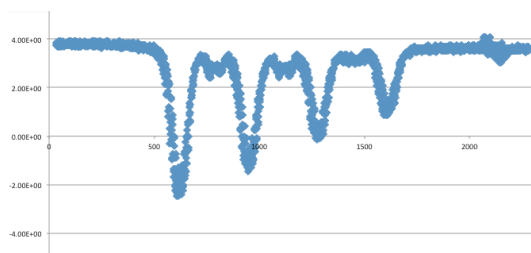

Figure 8: Energy level transitions in ^{85}Rb at 3.8MHz

From this graph, we can determine the relative energy spacings between the gaps.

5 CONCLUSION

My results are not yet fully conclusive as I believe I am missing a major factor in my figure comparing weak field RF frequency with the B field. Please suggest any possible errors that I could have made to get inaccurate slopes.

6 ACKNOWLEDGMENTS

References

[1] Fowles, Grant R. *Optical Pumping of Rubidium OP1-A: Guide to the Experiment INSTRUCTOR'S MANUAL*, 2002, TeachSpin, Inc.

[2] Black, Eric D. *Optical Pumping* Physics 77, Fall 2011, California Institute of Technology.